AIP | Applied Physics Letters

Suppression of vacancy aggregation by silicon-doping in low-temperature-grown Ga1−xCrxN

A. Yabuuchi, M. Maekawa, A. Kawasuso, Y.-K. Zhou, S. Hasegawa et al.

Citation: Appl. Phys. Lett. **102**, 142406 (2013); doi: 10.1063/1.4801426
View online: http://dx.doi.org/10.1063/1.4801426
View Table of Contents: http://apl.aip.org/resource/1/APPLAB/v102/i14
Published by the American Institute of Physics.

Suppression of vacancy aggregation by silicon-doping in low-temperature-grown $Ga_{1-x}Cr_xN$

A. Yabuuchi,[1,a)] M. Maekawa,[1] A. Kawasuso,[1] Y.-K. Zhou,[2] S. Hasegawa,[2] and H. Asahi[2]
[1]*Advanced Science Research Center, Japan Atomic Energy Agency, 1233 Watanuki, Takasaki, Gunma 370-1292, Japan*
[2]*The Institute of Scientific and Industrial Research, Osaka University, 8-1 Mihogaoka, Ibaraki, Osaka 567-0047, Japan*

(Received 23 January 2013; accepted 27 March 2013; published online 9 April 2013)

Effect of Si doping on low-temperature grown GaCrN films has been investigated by positron annihilation spectroscopy. In undoped GaCrN films grown at 540 °C, vacancy clusters with sizes of V_6–V_{12} were found to be responsible for positron trapping. Such vacancy clusters were considerably suppressed in Si-doped GaCrN films grown at 540 °C, although divacancies ($V_{Ga}V_N$) still survived. The Si-doping may be one possible way to suppress vacancy aggregation during low temperature crystal growth, and the further methods to remove divacancies are required. © *2013 American Institute of Physics*. [http://dx.doi.org/10.1063/1.4801426]

Transition-metal-doped semiconductors have attracted much attention as diluted magnetic semiconductor (DMS) materials.[1–4] For use in devices, high-Curie-temperature ferromagnetism is an important property. Among various DMSs, the Curie temperature of chromium-doped GaN has been reported to be higher than 400 K (Refs. 5 and 6) and hence a promising candidate operating at room temperature. In addition, GaN-based DMSs can also potentially emit blue light. The combination of the ferromagnetic and optical properties of GaCrN will lead to spintronic applications, such as circular polarization light emitting devices.

To exploit DMSs as spintronic devices, an improvement in magnetization per unit volume is necessary. Two approaches have been utilized in improving the magnetization:[7] Si-doping of GaCrN to enhance carrier-induced ferromagnetism and low temperature molecular beam epitaxy (MBE) growth to increase Cr atom concentration without formation of CrN precipitates. However, in the second method, GaCrN crystallinity will be degraded due to the introduction of vacancy defects during the MBE growth. These vacancy defects will act as carrier traps or non-radiative recombination centers. Maintaining crystallinity while suppressing vacancy defects in low-temperature growth is important for real device applications. In this study, vacancy defects in low-temperature-grown GaCrN films containing no secondary phases have been probed by a slow positron beam at different doping conditions.

Positron annihilation spectroscopy is a powerful technique to detect vacancy defects in crystalline solids.[8–10] In a perfect lattice, positrons annihilate at the interstitial region because positrons are repelled from ion cores. When vacancy defects exist, positrons tend to be trapped there and annihilate preferentially with valence electrons having lower momenta, compared to core electrons. Consequently, the intensity in the peak (tail) region of the Doppler broadening of annihilation radiation (DBAR) spectrum, that is associated mainly with valence (core) electrons, increases(decreases) as compared to the perfect lattice.[8–10]

The samples used in this study were GaN-cap (33 nm)/GaCrN (500 nm)/GaN-buffer (33 nm) structures. They were grown by a radio-frequency (RF) plasma-assisted MBE method on commercial GaN (2 μm)/Al_2O_3 (0001) templates grown by metal-oxide chemical vapor deposition (MOCVD). The GaN-buffer layers were prepared at 700 °C. The GaCrN (with Cr concentration of 0.7%) layers were grown at 540 °C with a growth rate of 200 nm/h. This growth temperature is low enough to prevent the CrN formation occurring at higher growth temperatures, e.g., 700 °C. The Ga flux, N_2 flow rate, RF plasma power, and Cr cell temperature were maintained constant at 1×10^{-7} Torr, 1.5 SCCM, 300 W, and 960 °C, respectively. Si-doped GaCrN film was also prepared. The Si cell temperature was set at 1100 °C. The cap layers were grown at 540 °C.

The crystallinity of the GaCrN samples was evaluated by X-ray diffraction (XRD) measurements. Monoenergetic positron beams with incident energy (E) of 0.2–25 keV were implanted into the samples, and the DBAR measurements were performed. The obtained DBAR spectra were characterized in terms of an S parameter, which is defined as the number of annihilation events over an energy range of 511 ± 0.8 keV divided by the total number of events in the 511 keV line. The value of S increases when positrons are trapped at vacancy defects. All the S parameters were normalized to that obtained from a MOCVD GaN template. To examine the electron-positron momentum distribution in detail, coincidence DBAR measurements were also performed.

To interpret experimental DBAR spectra, theoretical DBAR spectra were calculated within the local density approximation method.[11] The valence electron wavefunctions were calculated with the projector augmented-wave (PAW) method[12] using the ABINIT4.6.4 code.[13] The potentials and projectors were generated using the ATOMPAW code.[14] The valence electron configurations were $3d^{10}4s^24p^1$, $2s^22p^3$, $3s^23p^63d^54s^1$, and $3s^23p^2$ for Ga, N, Cr, and Si atoms, respectively. A supercell, including 32 Ga and 32 N atoms with a $2 \times 2 \times 2$ conventional wurtzite unit cell, was constructed as

a)Present address: Research Institute of Instrumentation Frontier (RIIF), National Institute of Advanced Industrial Science and Technology (AIST), 1-1-1 Umezono, Tsukuba, Ibaraki 305-8568, Japan. atsushi.yabuuchi@aist.go.jp

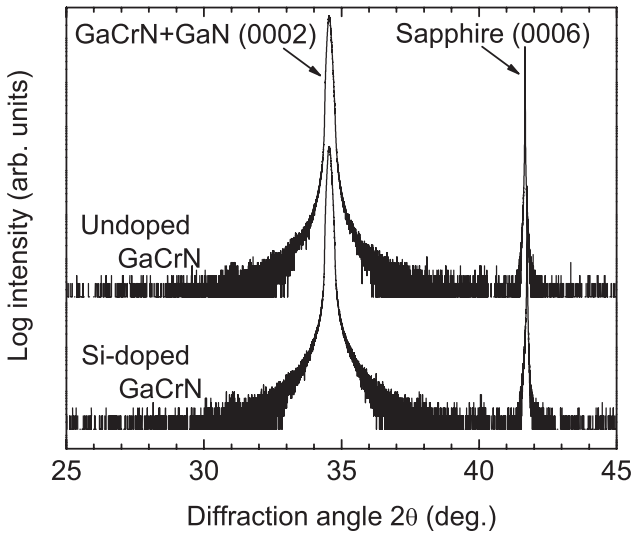

FIG. 1. XRD curves for the undoped and Si-doped GaCrN samples.

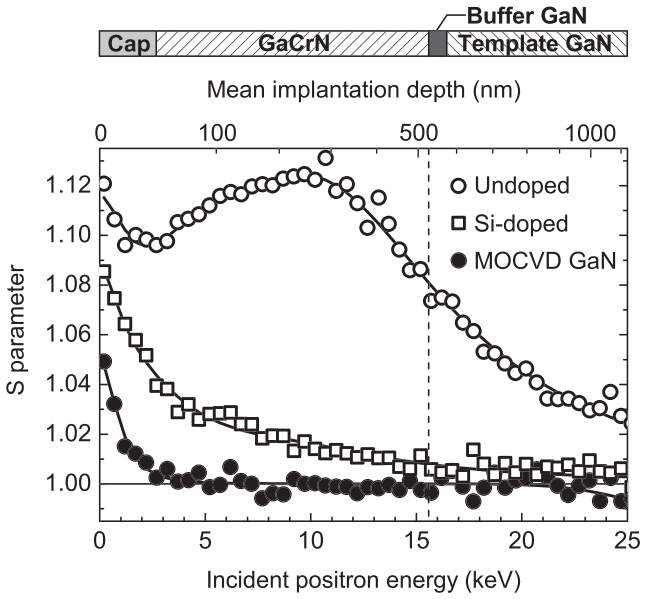

FIG. 2. *S* parameters as a function of incident positron energy obtained for undoped and Si-doped GaCrN samples. The *S* parameter of MOCVD GaN template is also plotted. All the *S* parameters are normalized to that obtained for MOCVD GaN. The upper horizontal axis denotes the average implantation depth corresponding to the incident positron energy. The top of the figure schematically shows the structure of the samples.

a GaN crystal. For vacancy defects, the lattice relaxations were introduced by the molecular dynamics simulation installed in the code. The cut-off energy of the plane wave basis set was 60 Ryd. The core electron wavefunctions were represented by the Slater function parameterized by Clementi and Roetti.[15] A self-consistent positron wavefunction was calculated based on the two-component density functional theory in order to minimize the energy functional.[16] The Borónski-Nieminen enhancement factor was adopted. The DBAR spectra were obtained by convoluting one-dimensional angular correlation of the annihilation radiation spectra obtained from the momentum density with the Gaussian resolution function having a half width of $3.92 \times 10^{-3} m_0 c$.

Figure 1 shows the XRD θ-2θ scan curves for the undoped and Si-doped GaCrN samples. Two diffraction peaks were observed at around 41.7° from sapphire (0006) and 34.6° from GaCrN and GaN (0002), respectively. No obvious secondary phase, such as CrN, was detected in these samples.

Figure 2 shows the *S* parameters for the undoped and Si-doped GaCrN samples as a function of incident positron energy. The increase in all *S* parameters in the low positron energy range ($E < 3$ keV) is related to surface effects, i.e., it is caused by positron annihilation or positronium formation at the sample surface.[17–19] *S* parameters at $3 < E < 15$ keV correspond to the GaCrN layers. The *S* parameter of the undoped GaCrN sample is significantly higher than that of the MOCVD GaN template suggesting the existence of vacancy clusters. Whereas, in the Si-doped GaCrN sample, the *S* parameter is considerably suppressed, although it is still higher than that of the MOCVD GaN template. These results indicate that the size and/or number of vacancy defects in the low-temperature-grown GaCrN are reduced by Si-doping. Probably, Si atoms, which occupy Ga sites as well as Ga vacancies,[20] reduce the size and/or number of vacancy defects.

Figure 3 shows the coincidence DBAR spectrum obtained for the MOCVD GaN template at $E = 8$ keV. The calculated DBAR spectra for perfect GaN lattice, Ga vacancy (V_{Ga}), and N vacancy (V_N) are also shown. The experimental spectrum is well reproduced by the theoretical curve for the perfect GaN lattice. The theoretical curve for V_{Ga} is sufficiently different from that for the perfect lattice. This means that at least the MOCVD GaN template does not contain vacancy defects, which are larger than Ga vacancies. The theoretical curve for V_N is rather similar to that for the perfect lattice. Therefore, although it is difficult to argue about the presence of N vacancies, the GaN template may be used as the reference sample.

Figures 4(c) and 4(d) show the coincidence DBAR spectra obtained for the undoped and Si-doped GaCrN samples at $E = 8$ keV. To see the detailed spectrum shape, the original spectra were normalized to that of the MOCVD GaN template. These measured DBAR spectra also indicate that

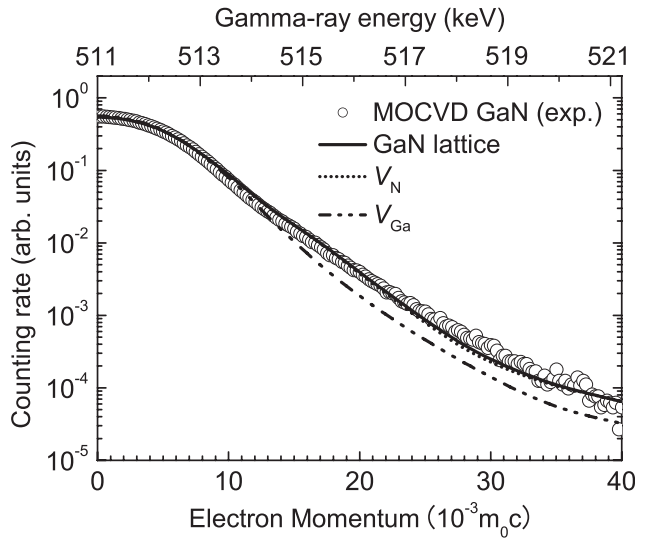

FIG. 3. Coincidence DBAR spectrum obtained for MOCVD GaN template at $E = 8$ keV. The calculated DBAR spectra for GaN lattice, Ga vacancy, and N vacancy are depicted by curved lines. The upper horizontal axis denotes the gamma-ray energy corresponding to the electron momentum.

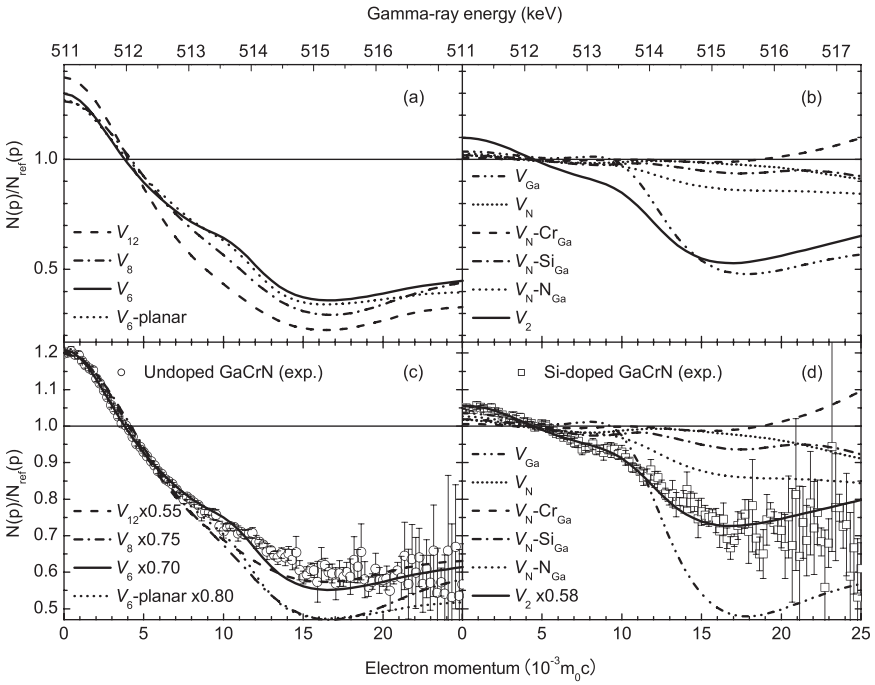

FIG. 4. Coincidence DBAR spectra obtained for (c) undoped and (d) Si-doped GaCrN films at $E = 8$ keV. The original measured spectra are normalized to the spectrum of MOCVD GaN. The calculated DBAR spectra for the various defect species are depicted by curved lines.

vacancy defects are present in both GaCrN samples. That is, an enhancement is seen in the low momentum region ($p < 5 \times 10^{-3} m_0 c$) and a suppression is observed in the high momentum region ($p > 10 \times 10^{-3} m_0 c$). In the spectrum of the Si-doped GaCrN sample, an additional shoulder is observed at around $p = 10 \times 10^{-3} m_0 c$. This shows that the defect species of the Si-doped GaCrN sample is different from that of the undoped one.

To characterize vacancy defects in the GaCrN samples, as shown in Figs. 4(a) and 4(b), the DBAR spectra were calculated assuming various defect species. These spectra are normalized to that of perfect GaN lattice. In the case of the undoped GaCrN sample [Fig. 4(c)], the experimental spectrum is not reproduced considering small vacancies shown in Fig. 4(b), because the amplitude of $N(p)/N_{\mathrm{ref}}(p)$ is significantly enhanced. This indicates that the size of the vacancy defects contained in the undoped GaCrN sample is larger than V_2. Therefore, we compare the experimental DBAR spectrum with larger vacancy clusters shown in Fig. 4(a). Here, V_6-planar denotes a six-membered ring-like vacancy cluster. In Fig. 4(c), the amplitudes of the calculated spectra for V_6, V_6-planar, V_8, and V_{12} around $N(p)/N_{\mathrm{ref}}(p)$ are adjusted to 0.70, 0.80, 0.75, and 0.55 times, respectively. The amplitude of the experimental spectrum is smaller than those of the calculated spectra for vacancy clusters. This indicates that only a part of implanted positrons localizes at vacancy clusters and the others delocalize in the lattice. The experimental spectrum is well reproduced with these calculation results. In particular, the experiment closely matches the calculated results for V_6 and V_{12}.

In covalently bound materials, such as semiconductors, vacancy clusters V_n that have particular magic numbers n have been reported to be stable, because a low number of dangling bonds (DBs) is considered to be favorable.[21–24] In wurtzite GaN crystals, V_2, V_4, V_6, V_8, V_{10}, and V_{12} defects have 6, 10, 10, 14, 18, and 18 DBs, respectively. This means that the total number of DBs is significantly reduced without increasing the number of DBs in each vacancy cluster by reactions of $V_4 + V_2 \rightarrow V_6$ or $V_{10} + V_2 \rightarrow V_{12}$. That is, the V_2, which has 6 DBs, can be eliminated by combining the V_2 with the V_4 (V_{10}), which has 10 DBs (18 DBs) and becoming the V_6 (V_{12}), which has the same 10 DBs (18 DBs). Hence, during crystal growth, V_4 and V_{10} defects will develop into more stable V_6 and V_{12} defects, respectively. This is also consistent with the prediction that the vacancy clusters V_n have particular magic numbers to minimize the number of DBs. From these results, the major positron trapping centers in the undoped GaCrN sample can be identified as vacancy clusters, and furthermore the observed experimental spectrum might be attributed to V_6 or V_{12}.

In the case of the Si-doped GaCrN sample [Fig. 4(d)], the experimental spectrum is not reproduced considering large vacancy clusters. We calculated the theoretical DBAR spectra assuming Ga vacancy (V_{Ga}), N vacancy (V_{N}), Ga-vacancy-Cr-impurity (V_{Ga}-$\mathrm{Cr_N}$), Ga-vacancy-Si-impurity (V_{Ga}-$\mathrm{Si_N}$), Ga-vacancy-Ga-antisite (V_{Ga}-$\mathrm{Ga_N}$), N-vacancy-Cr-impurity (V_{N}-$\mathrm{Cr_{Ga}}$), N-vacancy-Si-impurity (V_{N}-$\mathrm{Si_{Ga}}$), N-vacancy-N-antisite (V_{N}-$\mathrm{N_{Ga}}$) complexes, and divacancy (V_2). V_{Ga}-$\mathrm{Cr_N}$, V_{Ga}-$\mathrm{Si_N}$, and V_{Ga}-$\mathrm{Ga_N}$ complexes might not be potential candidates, because Cr and Si atoms have been reported to substitute Ga sites in GaN (Refs. 20 and 25) and a $V_{\mathrm{N}} \rightarrow V_{\mathrm{Ga}}$-$\mathrm{Ga_N}$ reaction cannot occur because the Ga-Ga bond is weaker than the Ga-N bond.[26] Therefore, the calculated spectra for V_{Ga}, V_{N}, V_{N}-$\mathrm{Cr_{Ga}}$, V_{N}-$\mathrm{Si_{Ga}}$, V_{N}-$\mathrm{N_{Ga}}$, and V_2 are depicted in Fig. 4(b) and compared with the experiment [Fig. 4(d)]. In Fig. 4(d), the amplitude of the calculated spectrum for V_2, around $N(p)/N_{\mathrm{ref}}(p)$, is also adjusted by 0.58 times. This again means that only a part of positrons was trapped at divacancies. Consequently, the experiment is found to be most well reproduced considering V_2. (The above-excluded candidates (V_{Ga}-$\mathrm{Cr_N}$, V_{Ga}-$\mathrm{Si_N}$, and V_{Ga}-$\mathrm{Ga_N}$ complexes) were also not compatible with the experiment.) Thus, the major positron trapping centers in the Si-doped GaCrN sample can be identified as divacancies.

Ga-site-substituted Si are proposed to trap second-nearest-neighbor Ga vacancies and consequently to form a V_{Ga}-Si_{Ga} complex.[27] The formation of the V_{Ga}-Si_{Ga} complexes will inhibit migration of V_{Ga} during crystal growth. Probably, this causes the suppression of vacancy aggregation, and as a result, the defects in the GaCrN layer stay in the form of divacancies.

In this study, defects in low-temperature-grown GaCrN samples have been investigated by positron annihilation spectroscopy. Vacancy clusters were detected in the undoped GaCrN sample. These vacancy clusters could be effectively removed by Si-doping; however, divacancies still survived. In addition to Si-doping for reducing vacancy clusters, post-growth annealing techniques for eliminating residual divacancies are needed to establish the low temperature growth technology of GaCrN films.

[1]H. Ohno, Science **281**, 951 (1998).
[2]S. A. Wolf, D. D. Awschalom, R. A. Buhrman, J. M. Daughton, S. von Molnár, M. L. Roukes, A. Y. Chtchelkanova, and D. M. Treger, Science **294**, 1488 (2001).
[3]Ü. Özgür, Y. I. Alivov, C. Liu, A. Teke, M. A. Reshchikov, S. Doğan, V. Avrutin, S.-J. Cho, and H. Morkoç, J. Appl. Phys. **98**, 041301 (2005).
[4]C. Liu, F. Yun, and H. Morkoç, J. Mater. Sci.: Mater. Electron. **16**, 555 (2005).
[5]M. Hashimoto, Y.-K. Zhou, M. Kanamura, and H. Asahi, Solid State Commun. **122**, 37 (2002).
[6]Y.-K. Zhou, M. Hashimoto, M. Kanamura, and H. Asahi, J. Supercond. Novel Magn. **16**, 37 (2003).
[7]Y.-K. Zhou, P. H. Fan, S. Emura, S. Hasegawa, and H. Asahi, Phys. Status Solidi C **9**, 719 (2012).
[8]P. Hautojärvi, *Positrons in Solids, Topics in Current Physics* (Springer, 1979).
[9]R. Krause-Rehberg and H. S. Leipner, *Positron Annihilation in Semiconductors, Solid-State Sciences* (Springer, 1999).
[10]P. G. Coleman, *Positron Beams and Their Applications* (World Scientific, 2000).
[11]M. J. Puska and R. M. Nieminen, Rev. Mod. Phys. **66**, 841 (1994).
[12]P. E. Blöhl, Phys. Rev. B **50**, 17953 (1994).
[13]X. Gonze, J.-M. Beuken, R. Caracas, F. Detraux, M. Fuchs, G.-M. Rignanese, L. Sindic, M. Verstraete, G. Zerah, F. Jollet, M. Torrent, A. Roy, M. Mikami, P. Ghosez, J.-Y. Raty, and D. C. Allan, Comput. Mater. Sci. **25**, 478 (2002).
[14]N. A. W. Holzwarth, A. R. Tackett, and G. E. Matthews, Comput. Phys. Commun. **135**, 329 (2001).
[15]E. Clementi and C. Roetti, At. Data Nucl. Data Tables **14**, 177 (1974).
[16]E. Borónski and R. M. Nieminen, Phys. Rev. B **34**, 3820 (1986).
[17]A. P. Mills, Jr., Phys. Rev. Lett. **41**, 1828 (1978).
[18]P. J. Schultz and K. G. Lynn, Rev. Mod. Phys. **60**, 701 (1988).
[19]P. Laukkanen, S. Lehkonen, P. Uusimaa, M. Pessa, J. Oila, S. Hautakangas, K. Saarinen, J. Likonen, and J. Keränen, J. Appl. Phys. **92**, 786 (2002).
[20]I. Halidou, Z. Benzarti, Z. Chine, T. Boufaden, and B. E. Jani, Microelectron. J. **32**, 137 (2001).
[21]D. J. Chadi and K. J. Chang, Phys. Rev. B **38**, 1523 (1988).
[22]Z. Tang, M. Hasegawa, T. Shimamura, Y. Nagai, T. Chiba, Y. Kawazoe, M. Takenaka, E. Kuramoto, and T. Iwata, Phys. Rev. Lett. **82**, 2532 (1999).
[23]T. E. M. Staab, M. Haugk, A. Sieck, T. Frauenheim, and H. S. Leipner, Physica B **273–274**, 501 (1999).
[24]T. E. M. Staab, M. Haugk, T. Frauenheim, and H. S. Leipner, Phys. Rev. Lett. **83**, 5519 (1999).
[25]M. Hashimoto, Y. K. Zhou, M. Kanamura, H. Katayama-Yoshida, and H. Asahi, J. Cryst. Growth **251**, 327 (2003).
[26]D. J. Chadi, Appl. Phys. Lett. **71**, 2970 (1997).
[27]U. Kaufmann, M. Kunzer, H. Obloh, M. Maier, C. Manz, A. Ramakrishnan, and B. Santic, Phys. Rev. B **59**, 5561 (1999).